Heat transfer by conduction, natural convection and radiation across a rectangular cellular structure

D. M. Kim and R. Viskanta*

This paper describes results on the effects of wall conduction and radiation heat exchange among surfaces on laminar natural convection heat transfer in a two-dimensional rectangular cavity modelling a cellular structure. Parametric heat transfer calculations have been performed, and numerical results are presented in graphical and tabular form. Local and average Nusselt numbers along the cavity walls are reported for a range of parameters of physical interest. The findings suggest that the local or the average Nusselt number is one of many parameters that control conjugate heat transfer problems. The results indicate that natural convection heat transfer in the cavity is reduced by heat conduction in the walls and radiation exchange among surfaces. The results obtained for the total heat transfer rate through the system using the two-dimensional model are compared with those based on a one-dimensional model.

Keywords: *heat transfer, convection, conduction, radiation*

There are numerous physical situations where heat is transported through solids which contain regularly or irregularly arranged cavities filled with air or other fluids. Examples of such situations include shells, sandwich structures, cellular materials such as bricks, insulations, cellular cavities, cement blocks, and foams[1]. Heat transfer through the structure or material is affected by the shape, size and number density of cavities (voids) through the structure, thermophysical properties of the solid and the fluid, the temperature level and imposed thermal conditions. In such situations heat transfer through the solid is by conduction and by combined natural convection and radiation across the cavity. Depending on the thermal conditions imposed on the system, either natural convection or thermal radiation may predominate. Heat transfer by conduction in the solid is affected by natural convection and radiation across the cavity and vice versa. Problems of this type are referred to as conjugate heat transfer problems and have received relatively little theoretical and experimental research attention.

Experimental and numerical computational studies dealing with natural convection in enclosures have been reported in the literature. Excellent reviews are available[2-4] and there is no need to repeat them. Most of the literature on natural convection heat transfer in cells and cavities does not account for wall heat conduction and radiation exchange between the walls. For example, heat conduction in an externally insulated wall causes the temperature distribution in the insulated wall to deviate from that of the adiabatic case, and thus precludes the possibility of obtaining experimentally a truly adiabatic boundary condition in some fluids such as air. In all enclosures thermal boundary conditions (wall conductance) can lead to stabilization or destabilization of the flow and corresponding large changes in the heat transfer coefficient. Natural convection in the cavity can also induce conduction heat transfer in the surrounding walls[5].

It has been recognized[4,5] that thermal boundary conditions (wall conduction and radiation exchange) on enclosure boundaries influence natural convection in the cavity but the problem has received relatively little theoretical and experimental attention[6-10]. Natural convection in a two-dimensional enclosure surrounded by one-dimensional conducting and radiating walls has been analyzed numerically[6]. The effects of cell wall thickness and thermal conductivity on natural convection heat transfer within inclined rectangular cavities have been analysed to gain understanding of the efficiency of cellular structures to reduce convective heat losses in flat-plate solar collectors[7,8]. Natural convection in a rectangular enclosure subjected to comparable horizontal and vertical temperature differences has been studied[9], and effects of finite wall heat conductance on natural convection in a two-dimensional rectangular cavity have been examined by solving numerically the model equations[10].

Solutions for natural convection heat transfer in rectangular cavities with perfectly insulated[11,13] and perfectly conducting[13-19] horizontal connecting walls have been reported. Natural convection in a cavity with a conducting insert has been analyzed using a finite element method[20]. A simplified analytical model for the computation of heat conduction across a rectangular-celled enclosure filled with a fluid has been presented, but the interaction between conduction in the walls and convection in the fluid has been neglected[21]. Analysis of heat

* Heat Transfer Laboratory, School of Mechanical Engineering, Purdue University, West Lafayette, IN 47907, USA
Received 5 January 1984 and accepted for publication on 2 July 1984

transfer in a prismatic rectangular bar cooled or heated by a flowing fluid in the circular cutouts of the bar has been performed and numerical results have been reported[22].

The purpose of this paper is to report on a computational study of heat transfer through cellular materials containing rectangular cavities. The results of the effects of wall conduction and radiation heat exchange on laminar natural convection heat transfer are investigated and quantified. A mathematical model is formulated, and numerical procedures are used to solve the model equations. Results of extensive parametric studies are reported in both graphical and tabular form. The results obtained are compared with predictions based on a simple one-dimensional model for overall heat transfer through the system.

Analysis

Physical model and assumptions

The physical model and coordinate system of the problem are shown in Fig 1. The two-dimensional, rectangular cavity or a module of a cellular structure containing numerous cavities is formed by walls having finite conductances. The vertical and the horizontal walls can be of different thickness but are assumed to be of the same material. Initially, the walls of the enclosure and the fluid inside the cavity are assumed to be at a constant, uniform temperature, and the fluid is taken to be stagnant. The horizontal connecting walls forming the enclosure are assumed to be insulated on the outside. At some time $t>0$ constant but different temperatures are suddenly imposed on the outside of the two vertical walls and maintained until steady-state conditions are reached.

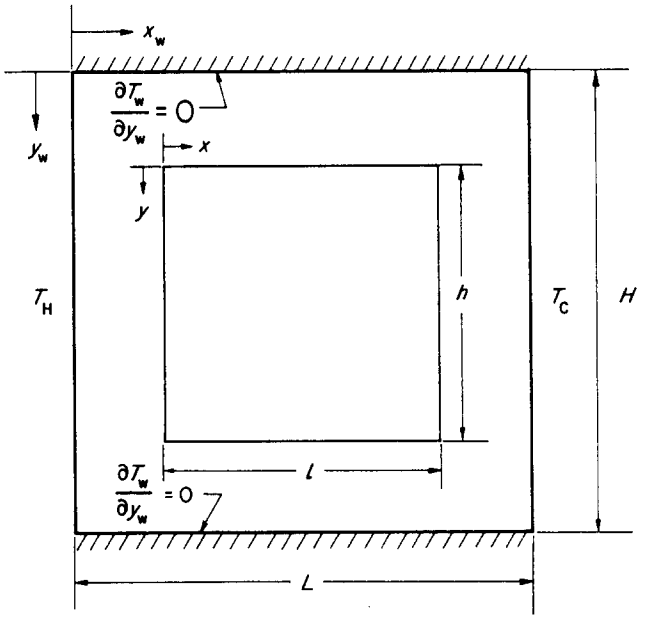

Fig 1 Physical model of the system

It is assumed in the analysis that the thermophysical properties of the walls and of the fluid are independent of temperature, except for the density in the buoyancy

Notation

AR	Aspect ratio of cavity, $\hbar/l$ (Fig 1)
F_{ij}	Configuration (view, angle) factor
H	Height of solid wall (Fig 1)
$\hbar$	Height of cavity (Fig 1)
h	Convective heat transfer coefficient
$\hbar^*$	Normalized cavity height, $\hbar/H$
J	Radiosity
J^*	Dimensionless radiosity, $J/\sigma T_H^4$
k	Thermal conductivity
k^*	Thermal conductivity ratio, k_w/k
L	Width of solid wall (Fig 1)
l	Width of cavity (Fig 1)
l^*	Normalized cavity width, l/L
N_r	Radiation number, $\varepsilon_w\sigma T_H^4 l/k_w(T_H-T_C)$
Nu	Local Nusselt number, hl/k
$\overline{Nu}$	Average Nusselt number, $\bar{h}l/k$
Pr	Prandtl number, ν/α
Q^*	Dimensionless, heat transfer rate, $\int_0^H q(x)dx/H(T_H-T_C)$
q	Heat flux
q_r^*	Dimensionless radiation heat flux, $q_r/\varepsilon_w\sigma T_H^4$
Ra	Rayleigh number, $g\beta(T_H-T_C)l^3/\nu\alpha$
Ra^*	Modified Rayleigh number, $g\beta(T_H-T_C)l^4/\nu\alpha L$
s	Position variable measured along the surfaces
T	Temperature
t	Time
U	Dimensionless velocity in the Y-direction, u/U_0
U_0	Reference velocity, α/l
u	Fluid velocity in the X-direction
V	Dimensionless velocity in the Y-direction, v/U_0
v	Fluid velocity in the Y-direction
x	Coordinate (Fig 1)
y	Coordinate (Fig 1)
α	Thermal diffusivity
α^*	Thermal diffusivity ratio, α_w/α
β	Thermal expansion coefficient
γ	Temperature ratio, T_H/T_C
ε	Emissivity
ζ	Dimensionless normal coordinate (ξ or ζ)
η	Dimensionless Y-coordinate, y/l
θ	Dimensionless temperature, $(T-T_C)/(T_H-T_C)$
ξ	Dimensionless X-coordinate, x/l
σ	Stefan-Boltzmann constant
τ	Dimensionless time, $\alpha t/l^2$
ϕ	Void fraction, hl/HL
Ψ	Dimensionless stream function, $\psi l/U_0$
ψ	Stream function
Ω	Dimensionless vorticity, $\omega l/U_0$
ω	Vorticity

Subscripts

b	Refers to bottom of cavity
C	Refers to the cold side of enclosure
c	Refers to cold side of cavity
H	Refers to the hot side of enclosure
h	Refers to hot side of cavity
i	Side of the wall
r	Radiation
t	Refers to top of cavity
w	Refers to solid wall

term. The fluid is Newtonian, incompressible, and the Boussinesq approximation is valid. Viscous heat dissipation in the fluid is assumed to be negligible in comparison to conduction and convection. The fluid motion and heat transfer in the cavity are assumed to be two-dimensional and laminar. The fluid inside the cavity is considered to be radiatively non-participating, and only radiation heat exchange among the gray diffusely emitting and reflecting walls is considered.

Model equations

For the sake of brevity, the conservation equations are written in dimensionless form from the start. The transient heat conduction equation in the wall is:

$$\frac{\partial\theta_w}{\partial\tau}=\alpha^*\left(\frac{l}{L}\right)^2\left[\frac{\partial^2\theta_w}{\partial\xi_w^2}+\left(\frac{L}{H}\right)^2\frac{\partial^2\theta_w}{\partial\eta_w^2}\right] \tag{1}$$

The conservation equations of mass, momentum and energy for the fluid can be expressed in standard form by introducing the concepts of stream function and vorticity. The dimensionless vorticity, stream function, energy and velocity equations become, respectively:

$$\frac{\partial\Omega}{\partial\tau}+\left[\frac{\partial(U\Omega)}{\partial\xi}+\frac{1}{AR}\frac{\partial(V\Omega)}{\partial\eta}\right]=Pr\left(\frac{\partial^2\Omega}{\partial\xi^2}+\frac{1}{AR^2}\frac{\partial^2\Omega}{\partial\eta^2}\right)+Ra^*Pr\frac{\partial\theta}{\partial\xi} \tag{2}$$

$$\frac{\partial\theta}{\partial\tau}+\frac{\partial(U\theta)}{\partial\xi}+\frac{1}{AR}\frac{\partial(V\theta)}{\partial\eta}=\frac{\partial^2\theta}{\partial\xi^2}+\frac{1}{AR^2}\frac{\partial^2\theta}{\partial\eta^2} \tag{3}$$

$$\Omega=-\left[\frac{\partial^2\Psi}{\partial\xi^2}+\frac{1}{AR^2}\frac{\partial^2\Psi}{\partial\eta^2}\right] \tag{4}$$

where the velocities are defined in terms of the stream function as:

$$U=\frac{1}{AR}\frac{\partial\Psi}{\partial\eta}\qquad\text{and}\qquad V=-\frac{\partial\Psi}{\partial\xi} \tag{5}$$

The initial temperature in the system is assumed to be uniform and the fluid is stagnant. The vertical outside walls of the enclosure are at constant but different temperatures and the horizontal connecting walls are insulated. At the interior walls (solid–fluid interface) of the enclosure there is no slip; the temperature is continuous, ie $\theta(\xi,\eta,\tau)_w=\theta_w(\xi,\eta,\tau)_w$. A local energy balance at the inside surface of a wall gives the condition:

$$-\frac{\partial\theta_w}{\partial\zeta}=-\frac{1}{k^*}\frac{\partial\theta}{\partial\zeta}+N_r q_r^* \tag{6}$$

where the local radiative heat flux at any surface i can be expressed as:

$$q_{ri}^*=\left(1-\frac{1}{\gamma}\right)^4\left(\theta_i+\frac{1}{\gamma-1}\right)^4-\sum_{j=1}^{4}\int_{A_j}J_j^*(s_j)K(s_i,s_j)\mathrm{d}A_j\qquad i,j=1,2,\ldots,4 \tag{7}$$

For the sake of brevity the integral equations for the radiosities J_j^* are not given here, but they can be found elsewhere[6,23]. Even though the wall emissivity does not appear directly in the expressions for the local radiative fluxes q_{ri}^* because of the nondimensionalization used, it is present as a parameter in the radiosity equations J_i^*.

The convective heat transfer coefficient h is based on $(T_H+T_C)/2$ as the reference temperature since a meaningful fluid temperature cannot be defined. Using the dimensionless variables, the local Nusselt number can be expressed as:

$$Nu=-\left.\frac{\partial\theta}{\partial\xi}\right|_w \tag{8}$$

Method of solution

Analytical solutions of the governing conservation equations are not feasible, and approximate methods available are not sufficiently flexible. Therefore, a numerical method has been adopted. The various schemes which are available[24,25] will not be discussed here. The alternating direction implicit (ADI) method[24] has been adopted for the numerical solution of the system of equations, Eqs (1)–(4), together with the boundary conditions. For this purpose the stream function equation, Eq (4), was also rewritten in a transient form and solved using the ADI method until steady-state was reached[6].

A uniform grid spacing was used in the solid wall. However, in order to resolve the boundary layers in the fluid it was desirable to use a non-uniform mesh for accuracy and computational efficiency. The temperature field in the solid and the velocity and temperature fields in the fluid are computed as a function of time. However, only the steady state results are reported in the paper as they are of primary interest.

The effect of the total number of nodes and the number of nodes in the fluid have been examined, and the results reported here have been obtained using 26×26 grid for the enclosure with 16×16 grid in the fluid. The numerical results agreed well with the benchmark solutions for limiting cases[11,12,18]. For $Ra=10^6$ and $Ra=10^7$ the average Nusselt numbers calculated differed from the benchmark solutions[11] by a maximum of 1.5% and 2.2% respectively.

Validation of the model and of the numerical scheme was also achieved by successfully predicting the interferometrically measured temperature distributions for a square cavity filled with atmospheric pressure air[23]. Numerical experiments performed with different grids showed that the number of nodes chosen was a reasonable compromise between computational effort and accuracy. For example, there was less than 0.022% difference between the average Nusselt numbers calculated using 13×13 and 21×21 grids in the fluid for a Rayleigh number of 10^6.

One-dimensional heat transfer model

If heat transfer is predominantly one-dimensional, the rate through the system can be estimated using the thermal resistance concepts[26]. Assuming one-dimensional heat transfer and no interaction between conduction in the solid and natural convection-radiation with the adiabatic (reradiating) connecting horizontal walls, the total heat transfer rate can be expressed in dimensionless form as:

$$Q^*=Q/[k_wLH(T_H-T_C)/L]=(1-\mathcal{A}^*)+(1/l^*)^2\Phi/[k^*/\tilde{N}u+(1/l)-1] \tag{9}$$

where:

$$\tilde{N}u=\frac{(\bar{h}+\bar{h}_r)\ell}{k}=\overline{Nu}+\overline{Nu}_r \tag{10}$$

The convective heat transfer coefficient $\bar{h}$ for the cavity can be evaluated from the correlations available in the literature which neglect the interaction between conduction in the wall and natural convection in the fluid[11-17]. The effective radiative heat transfer coefficient $\bar{h}_r$ is found to be:

$$\bar{h}_r=\sigma(T_h^3+T_h^2T_c+T_hT_c^2+T_c^3)\Big/\left[2\left(\frac{1-\varepsilon_w}{\varepsilon_w}\right)+\frac{1}{\bar{F}_{h-R}}\right] \tag{11}$$

where $\bar{F}_{h\text{-}R}$ is a radiation exchange factor which accounts for the presence of adiabatic (reradiating) horizontal connecting walls[26].

Note that the radiative resistance $1/\bar{h}_r$ cannot be determined without the knowledge of the heat transfer rate across the cavity since the temperatures T_h and T_c at the cavity surfaces are not known. However, T_h and T_c can be calculated by linear approximation from the outside wall temperatures T_H and T_C ($T_h=[T_H(L+l)+T_C(L-l)]/2L$ and $T_c=T_C+(L-l)(T_H-T_C)/2L$). Hence, an iterative procedure must be used to calculate the radiative heat transfer coefficient h_r and the heat transfer rate through the system.

Results and discussion

There are a large number of independent parameters (Ra^*, Pr, AR, H/L, ϕ, k^*, α^*, ε_w, N_r, and γ) governing the problem and it is not feasible to obtain solutions for the complete range of interest. Solutions have been obtained for combined conduction, radiation and laminar natural convection in cavities with all four walls having finite conductances. The results for the flow and temperature fields, the local Nusselt numbers, the average Nusselt numbers, and total heat transfer through the system are calculated for different Prandtl number fluids over a modified Rayleigh number Ra^* range from 10^4 to 10^7 and specific values of L/H, AR, ϕ, k^*, α^*, N_r, ε_w, and γ. The emphasis of the discussion in the paper is on heat transfer rather than on stability or flow.

Heat transfer in the absence of radiation

Isotherms and flow fields

Extensive numerical results for flow and temperature fields have been obtained for different Ra^*, ϕ, AR, and Pr in the cavity[23]. Suffice it to mention that the results are similar to those obtained by others in the absence of wall conduction[11-20]. Presence of conduction can simultaneously stabilize and destabilize the fluid in the cavity and affects both the temperature distribution and convective heat transfer at the walls.

Local and average Nusselt numbers

Because the system considered has four conducting walls, the local Nusselt numbers should be defined for all four walls. Fig 2 shows the effect of the Rayleigh number on the local heat transfer along the hot vertical and horizontal connecting walls, respectively. As a result of the definitions adopted, the local Nusselt number is positive if heat flows from the wall to the fluid, and negative if heat flows from the fluid to the wall. At the connecting horizontal walls the local Nusselt number does not vanish and may be either positive or negative, depending on the position along the walls. This indicates that for conjugate (combined conduction-convection-radiation exchange) problems the Nusselt number may not be the most desirable heat transfer parameter for correlating results and data. For the problem considered, the Nusselt number not only depends on the geometry of the cavity and the relevant conventional parameters (Ra and Pr) but also on the thermophysical properties of the wall materials (α^* and k^*), the porosity (ϕ), and the geometry of the cavity within the enclosures (L/H and AR).

The maximum local Nusselt number at the hot vertical wall (Fig 2) occurs in the lower half of the cavity ($\eta\approx0.7$). This is caused by the cold fluid, which descended from the cold wall, moved along the connecting wall, and impinged on the hot wall near its base. It is interesting to note the change of heat flow direction at the horizontal connecting walls. The location along the wall where the direction of heat flow is reversed depends on the modified Rayleigh number, Prandtl number and other parameters (ϕ, AR, L/H, and k^*)[23].

The effects of the porosity ϕ and the aspect ratio AR on the local Nusselt number at the heated wall are shown in Figs 3 and 4 respectively. The Nusselt number depends strongly on both the void fraction and on the aspect ratio. The local Nusselt numbers with $\phi=0.5$ are almost twice as large as the ones for $\phi=0.25$ for the same Rayleigh numbers (Fig 3). This is due to the larger temperature difference across the cavity between the hot

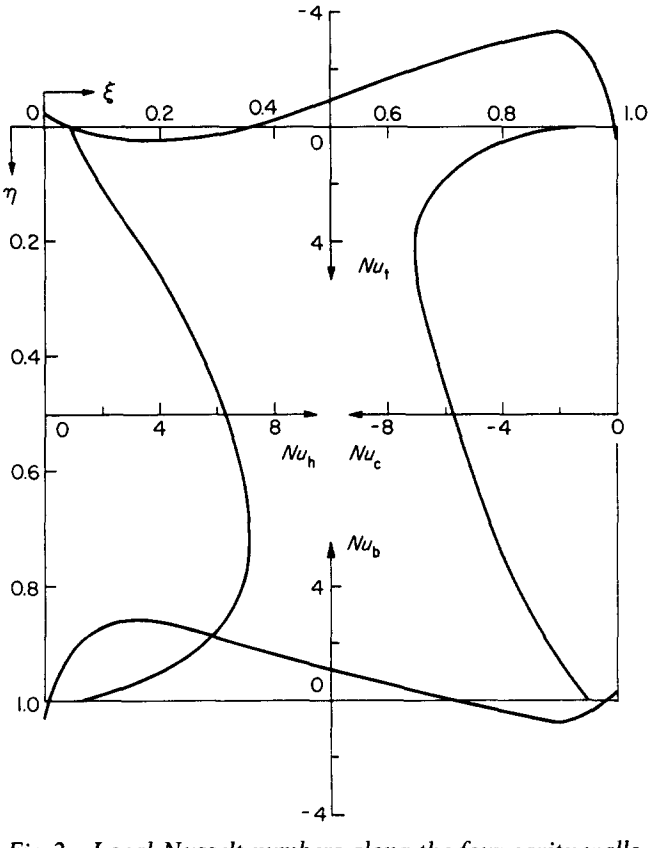

Fig 2 Local Nusselt numbers along the four cavity walls ($Ra^*=10^6$, $Pr=0.71$, $AR=1.0$, $H/L=1.0$, $\phi=0.5$, $k^*=10.0$, $\alpha^*=0.005$, *and* $N_r=0$)

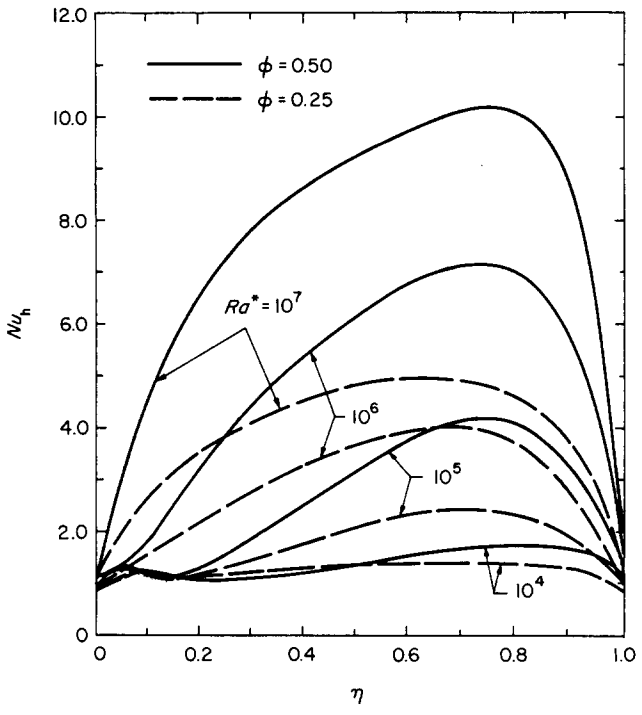

Fig 3 Effect of void fraction on the local Nusselt number (Pr=*0.71*, AR=*1.0*, L/H=*1.0*, ϕ=*0.5*, k*=*10.0*, *and* α^*=*0.005*)

and cold inside walls which increase with the void fraction, resulting in more intense natural convection circulation in the cavity. Fig4 shows that the effect of Rayleigh number on the local Nusselt number is much more significant for $AR=0.5$ than for $AR=2.0$. The location of the maximum value of Nu_h occurs in the lower half of the cavity ($\eta \approx 0.7$) and is affected little by Ra^*.

The results for the average Nusselt number have been calculated for a range of modified Rayleigh numbers and are given in Table 1. As the modified Rayleigh number increases, the average Nusselt number on the four walls of the cavity also increases. Although the average Nusselt numbers at the top and the bottom walls are quite small, the local Nusselt numbers can be quite large (Fig 2). In other words, the total heat transfer across the top and bottom walls of the cavity is small since the average Nusselt number is very small at the top and the bottom of the cavity, but the local heat transfer through the top and the bottom walls is large.

An empirical correlation of the average Nusselt number for a rectangular cavity surrounded by conducting wall has been obtained from a least squares fit of the numerical results:

$$\overline{Nu} = 0.410\phi^{0.93}(k^*)^{0.138}(Ra^*)^{0.2} \qquad 0.3 < Pr < 50 \qquad (12)$$

$$\overline{Nu} = 0.485\phi^{0.93}(k^*)^{0.138}(Ra^*)^{0.2} \qquad 50 < Pr < 100 \qquad (13)$$

These equations are based on the following range of parameters: $10^5 < Ra^* < 10^7$, $0.25 < \phi < 0.6$, $3 < k^* < 100$, and $AR = 1.0$. A comparison of average Nusselt numbers between the correlations, Eqs (12) and (13), for finite conductance walls and the correlations for the limiting case of isothermal cavity with perfectly conducting and perfectly insulated horizontal walls is of interest. A correlation for the average Nusselt number at the heated wall for the case of perfectly insulated horizontal connecting walls has been obtained from the least squares fit of the numerical data of the form:

$$\overline{Nu} = 0.126Ra^{0.31} \qquad 5 \times 10^3 < Ra < 10^7 \qquad (14)$$

The correlation gives a maximum error of 3% in comparison with the benchmark solutions[11] for $10^4 < Ra < 10^6$, and 2% error in comparison with other published results[12] for $Ra = 10^7$. A correlation of the average Nusselt number at the heated vertical wall for perfectly conducting horizontal connecting walls has also been obtained from a least squares fit of the numerical results in the form:

$$\overline{Nu} = 0.129Ra^{0.283} \qquad 10^4 < Ra < 5 \times 10^6 \qquad (15)$$

The correlation gives a maximum error of 2% in comparison to the reported solution[17] for $10^4 < Ra < 10^5$ and also to the other results[13] for $Ra = 10^6$.

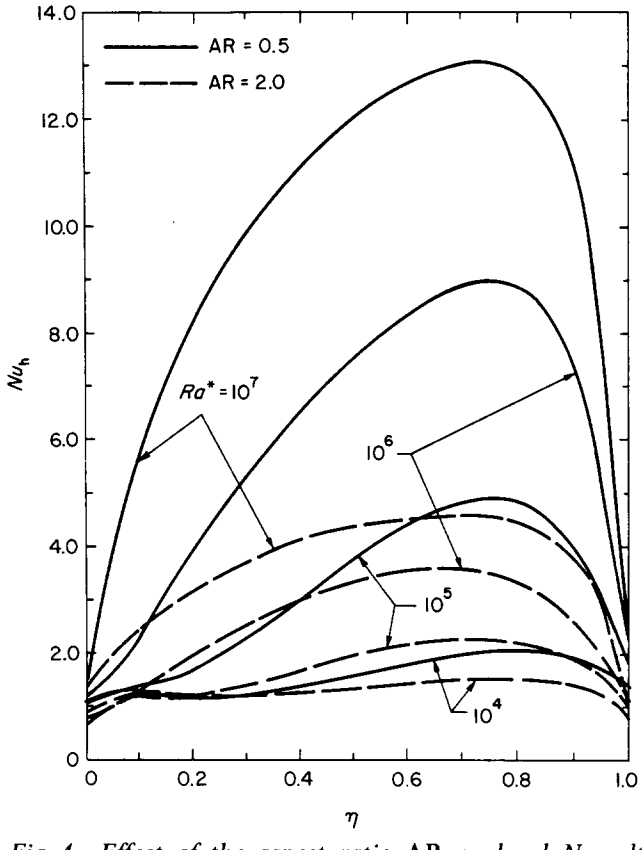

Fig 4 Effect of the aspect ratio AR *on local Nusselt number at the hot wall* (Pr=*0.71*, AR=*0.5*, L/H=*1.0*, ϕ=*0.36*, k*=*10.0*, *and* α^*=*0.005*)

Table 1 Average Nusselt number along the four walls of a square cavity; Pr=0.71, AR=1.0, H/L=1.0, ϕ=0.36, k^*=10.0, and α^*=0.005

	Average Nusselt number			
Ra*	$\overline{Nu}_h$	$\overline{Nu}_c$	$\overline{Nu}_t$	$\overline{Nu}_b$
10^4	1.310	1.311	0.219	0.220
10^5	2.195	2.184	0.651	0.647
10^6	3.801	3.781	1.017	1.057
10^7	5.517	5.701	−1.139	1.555

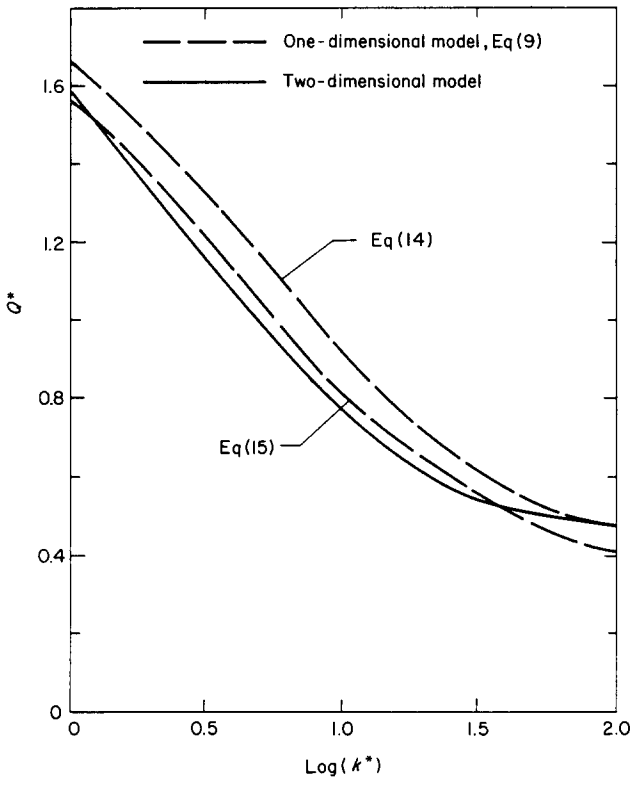

Fig 5 Comparison between the one- and two-dimensional models for the total heat transfer across the system (Ra* = *10⁶*, Pr = *0.71*, AR = *1.0*, L/H = *1.0*, ϕ = *0.36*, α^* = *0.005*, *and* N_r = *0*)

Total heat transfer

The temperature gradient in the solid becomes smaller with an increase in the thermal conductivity ratio, and as a result, the dimensionless total heat transfer rate decreases as k^* increases (Fig 5). This indicates that the thermal conductivity ratio becomes a more dominant parameter than natural convection (Nusselt number) in controlling the total heat transfer rate through the system. The rate depends not only on the Nusselt number, but is also strongly dependent on the thermal conductivities of the solid and the fluid. The comparison between the results obtained with the one-dimensional, using either Eq (14) or Eq (15) for $\overline{Nu}$, and the two-dimensional models for the total heat transfer rate with the thermal conductivity ratio k^* as a parameter indicates that the effect of natural convection on the total heat transfer becomes significant as the thermal conductivity ratio decreases. The one-dimensional model — Eq (9) with Eq (14) for $\overline{Nu}$ — overpredicts the total heat transfer rate by 6% at $k^* = 10$. However, the one-dimensional model — Eq (4) with Eq (15) for $\overline{Nu}$ — underpredicts the total heat transfer by 14% at $k^* = 100$. This indicates that when heat conduction predominates over natural convection, the one-dimensional model accurately predicts the total heat transfer for large thermal conductivity ratios.

Fig 6 shows a comparison of total heat transfer predictions based on the one-dimensional (with Eq (15) for $\overline{Nu}$) and on the two-dimensional models for different void fractions. As the Rayleigh number increases, the effect of natural convection on the total heat transfer rate becomes more significant for higher void fractions. The one-dimensional model underpredicts the total heat transfer at lower modified Rayleigh number and overpredicts at higher Rayleigh number ($Ra^* > 10^5$).

The total heat transfer rates have been calculated for different aspect ratios and are presented and compared in Fig 7 with the results based on the one-dimensional model described earlier. The average Nusselt number correlations used for the three different aspect ratio cavities are indicated in the figure. The dimensionless total heat transfer rate is increased with a decrease in the aspect ratio. This clearly indicates that the aspect ratio is an important parameter which influences the heat transfer through the system. The effect of heat conduction on the total heat transfer is significant at the low modified Rayleigh numbers, but natural convection becomes the important heat transfer mode at higher Rayleigh numbers for aspect ratio of 0.5. This means that the one-dimensional model can accurately predict the total heat transfer rate at low Rayleigh number. However, for higher Rayleigh number with $AR = 0.5$ or greater, the model does not accurately predict the total heat transfer rate.

Heat transfer with radiation interchange among cavity walls

Flow and temperature fields

When radiation exchange among cavity walls is accounted for, three additional parameters, radiation number N_r, wall emissivity ε_w, and temperature ratio γ, arise and must be considered together with wall heat conduction parameters. Increase in the radiation parameter N_r and an increase in the surface emissivity of the cavity wall ε_w increase the temperature drop through the vertical walls of the system and the temperature gradients in the fluid

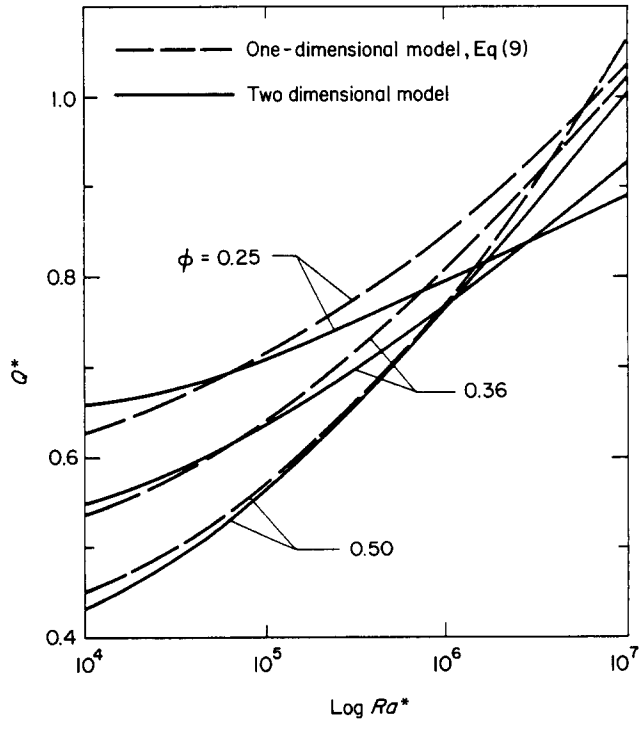

Fig 6 Effect of void fraction of the total heat transfer across the system (Pr = *0.71*, AR = *1.0*, L/H = *1.0*, k* = *10.0*, α^* = *0.005 and* N_r = *0*)

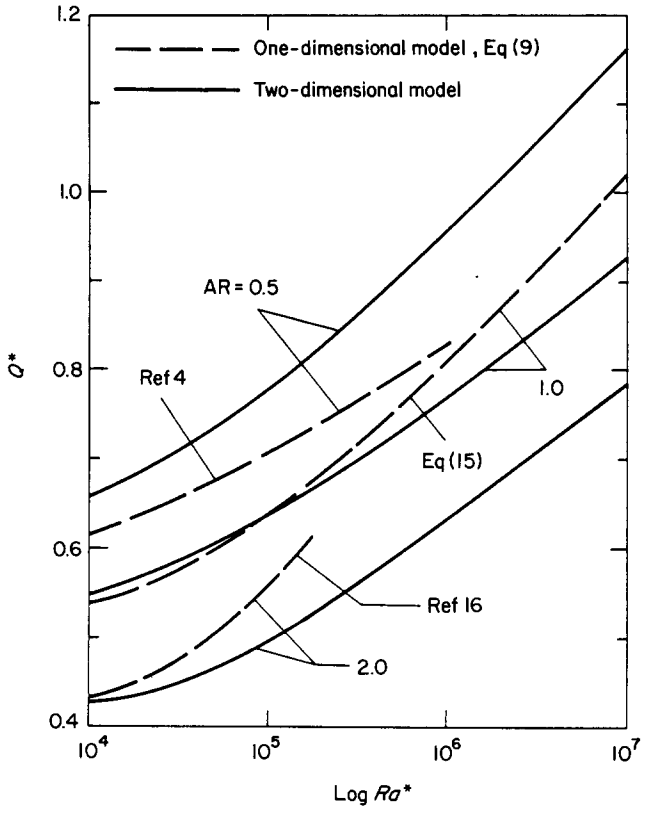

Fig 7 Effect of aspect ratio on the total heat transfer across the system (Pr = *0.71*, ϕ = *0.36*, L/H = *1.0*, k* = *10.0*, α^* = *0.005 and* N_r = *0*)

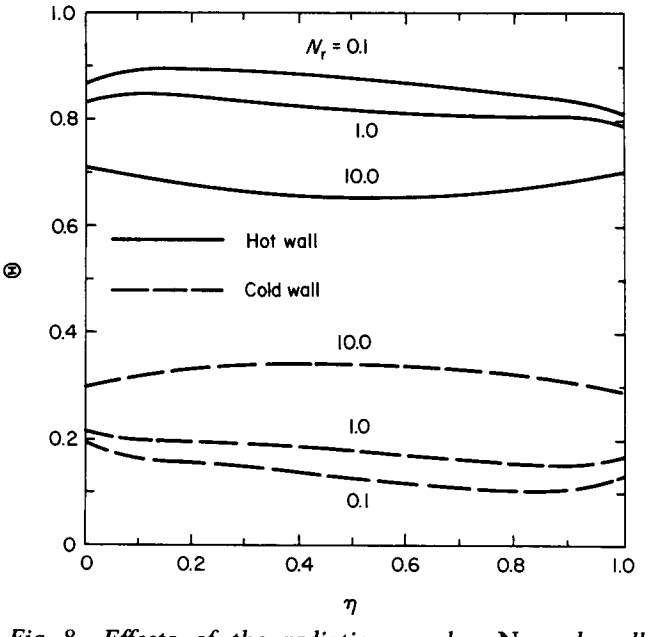

Fig 8 Effects of the radiation number N_r *and wall emissivity* ε_w *on the temperature distribution in the vertical wall* (Ra* = 10^6, Pr = *0.71*, AR = *1.0*, H/L = *1.0*, ϕ = *0.36*, k* = *10.0*, α^* = *0.005*, γ = *1.2, and* ε_w = *1.0*)

near the walls. This results in significantly lower temperature across the cavity (Fig 8) than when radiation was absent. The reduced temperature difference between the hot and cold inside surfaces of the cavity results in a decrease of the buoyancy force. The stream function at the midpoint decreases from $\Psi_0 = 16.35$ ($N_r = 1$ and $\varepsilon_w = 1.0$) to $\Psi_0 = 14.32$ ($N_r = 10$ and $\varepsilon_w = 1.0$). This means that natural convection circulation becomes less intense with an increase in radiation heat transfer. However, the stream function at the midpoint of the cavity changes little — from $\Psi_0 = 16.41$ ($\varepsilon_w = 0$ and $N_r = 1$) to $\Psi_0 = 16.34$ ($\varepsilon_w = 1.0$ and $N_r = 1$) — as the wall emissivity is increased. The effects of radiation on the vertical velocities are not significant as the radiation number is changed from $N_r = 0.1$ to 1, but are more pronounced as the radiation number is changed from $N_r = 1$ to 10.

Local and total heat transfer

The dimensionless local heat fluxes at the hot and the cold inside walls show that radiation heat transfer predominates over natural convection for $N_r = 10$, and for a given radiation number N_r the flux increases as the wall emissivity is increased. The flux is relatively uniform along the vertical walls, except near the top and the bottom of the walls[23].

Fig 9 shows the local Nusselt number variation along the hot vertical wall for different radiation parameters N_r and wall emissivities ε_w. The local convective heat transfer decreases significantly as the radiation parameter N_r is increased and indicates that radiation heat exchange predominates over natural convection. The local Nusselt number decreases with an increase in the wall emissivity ε_w as a result of decreasing temperature gradient in the fluid.

The percentage of the total heat transfer at $\xi_w = 0.2$ (ie vertical plane corresponding to the hot inside vertical surface) is given as a function of wall emissivity ε_w in Table 2. The percentages of heat transfer by conduction and natural convection are 51.4% and 48.6%, respectively, for the perfectly reflecting wall ($\varepsilon_w = 0$). However, these percentages decrease to 44.0% and 35.5%, respectively, for a

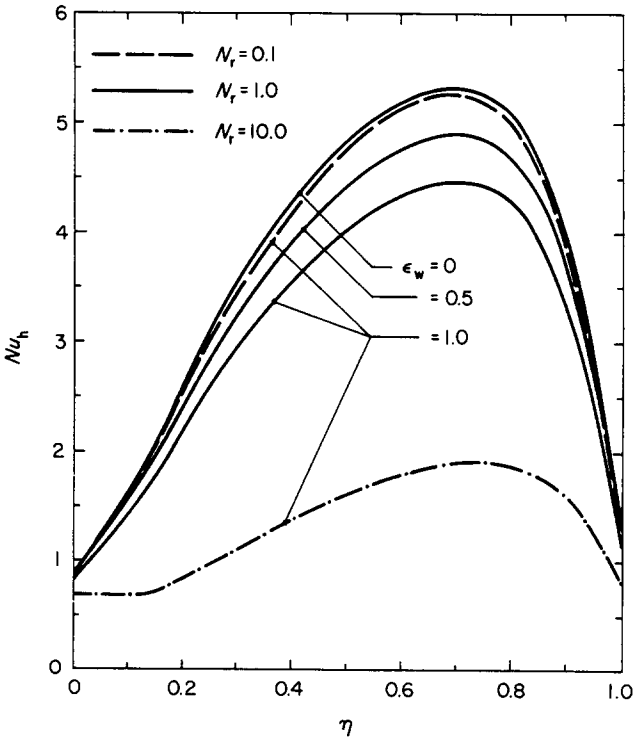

Fig 9 Effects of the wall emissivity ε_w *on the local Nusselt number* (R*a = 10^6, Pr = *0.71*, AR = *1.0*, H/L = *1.0*, k* = *10.0*, α^* = *0.005*, γ = *1.2, and* N_r = *0*)

Table 2 Effect of wall emissivity ε_w on the fraction of the total heat transfer at the plane; $\xi_w=0.2$, $Ra^*=10^6$, $N_r=1.0$, and $\gamma=1.2$

ε_w	0	0.25	0.5	0.75	1.0
Q_{cond}, %	51.4	48.9	47.2	45.5	44.0
Q_{conv}, %	48.6	45.4	41.5	38.1	35.5
Q_{rad}, %	0	5.7	11.3	16.4	20.5

Table 3 Effect of radiation heat transfer on average Nusselt number and total dimensionless heat transfer; $Pr=0.71$, $AR=1.0$, $H/L=1.0$, $\phi=0.36$, $\alpha^*=0.005$, $k^*=10.0$, $\varepsilon_w=1.0$, $\gamma=1.2$, and $N_r=1.0$

Ra^*	10^4	10^5	10^6	10^7
$\overline{Nu}_h$	1.112 (1.310)	1.382 (2.195)	3.210 (3.801)	4.902 (5.517)
Q^*	0.708 (0.548)	0.807 (0.638)	0.941 (0.771)	1.042 (0.928)

Table 4 Effect of wall emissivity ε_w on average Nusselt number and total dimensionless heat transfer; $Ra^*=10^6$, $Pr=0.71$, $AR=1.0$, $H/L=1.0$, $\phi=0.36$, $\alpha^*=0.005$, $k^*=10.0$, $N_r=1.0$, $\gamma=1.2$

ε_w	0.0	0.25	0.5	0.75	1.00
$\overline{Nu}_h$	3.801	3.688	3.523	3.358	3.210
Q^*	0.773 (0.815)	0.834 (0.848)	0.879 (0.886)	0.915 (0.926)	0.941 (0.971)

black wall ($\varepsilon_w=1.0$). Radiation heat transfer accounts for about 20% of the total heat transfer when the wall is black ($\varepsilon_w=1.0$).

Table 3 shows the effect of radiation on the total heat transfer for various modified Rayleigh numbers and compares the results for a model without radiation (given in parentheses). The dimensionless heat transfer rate calculated as a function of the wall emissivity ε_w, radiation number N_r, and imposed temperature ratio is shown in Tables 4, 5 and 6, respectively. The total heat transfer rates predicted by the one-dimensional model are shown in parentheses in Tables 4 and 5. The total heat transfer rate through the structure depends strongly on the wall emissivity, radiation number, and the imposed temperature ratio rather than the average Nusselt number. The Nusselt number is thus seen to be one of many parameters that controls the heat transfer rate in conjugate heat transfer problems.

Conclusions

Based on the numerical results obtained, the following conclusions can be drawn:

1. In an unstable arrangement such as heating from the side, heat conduction in the walls and radiation exchange among walls reduce the driving force for natural convection as well as producing thermal stratification in some regions of the cavity.

Table 5 Effect of radiation number N_r on average Nusselt number and total dimensionless heat transfer; $Ra=10^6$, $Pr=0.71$, $AR=1.0$, $H/L=1.0$, $\phi=0.36$, $k=10.0$, $\alpha=0.005$, $\gamma=1.2$, and $\varepsilon_w=1.0$

N_r	0.01	0.1	1.0	10.0	50.0
$\overline{Nu}_h$	3.801	3.773	3.210	1.379	0.392
Q^*	0.773 (0.815)	0.795 (0.835)	0.941 (0.971)	1.577 (1.451)	1.965 (1.785)

Table 6 Effect of the imposed temperature ratio γ on average Nusselt number and total dimensionless heat transfer; $Ra^*=10^6$, $Pr=0.71$, $AR=1.0$, $H/L=1.0$, $\phi=0.36$, $k^*=10.0$, $\alpha^*=0.005$, $N_r=1.0$, and $\varepsilon_w=1.0$

γ	1.05	1.15	1.2	2.0	5.0	10.0
$\overline{Nu}_h$	3.608	3.308	3.210	2.826	2.852	2.892
Q^*	0.837	0.916	0.941	1.038	1.021	1.006

2. The Nusselt number is only one of many parameters that control heat transfer in conjugate problems. The total heat transfer rate depends not only on the natural convection in the cavity but also on the wall conductances and the radiation parameters.

3. The Nusselt number at the heated vertical wall increases with a decrease in the wall emissivity ε_w, radiation number N_r, and imposed temperature ratio γ and increases with the modified Rayleigh number Ra^*, and the Prandtl number Pr.

4. Total heat transfer through the system depends not only on the Nusselt number in the cavity, as influenced by the Rayleigh number, but also on the thermophysical properties of the wall material and the fluid, and the parameters governing radiation exchange among the cavity walls.

5. The one-dimensional model for heat transfer across the cellular enclosure which ignores the interaction between wall heat conduction and natural convection in the cavity yields a reasonable prediction (within $\pm 20\%$) of the total heat transfer in comparison with the detailed two-dimensional model.

References

1. **Jakob M.** *Heat Transfer, vol. 1, pp. 82–107, John Wiley, New York, 1949*
2. **Catton I.** Natural convection in enclosures, *Heat Transfer — 1978, 6, 13–30, Natural Research Council of Canada, Ottawa, 1978*
3. **Ostrach S.**, Natural convection heat transfer in cavities and cell. *Heat Transfer 1982, vol. 7, 365–379, Hemisphere Publishing Corp., Washington, DC, 1982*
4. **Catton I., Bejan A., Greif R. and Hollands K. G. T.** Natural Convection in Enclosures. *Proceedings of Workshop on Natural Convection (eds K. T. Yang and J. R. Lloyd), University of Notre Dame, Notre Dame, Indiana, 1983, 24–35*
5. **ElSherbiny S. M., Hollands K. G. T. and Raithby G. D.** Effect of thermal boundary conditions on natural convection in vertical

and inclined air layer. *ASME J. Heat Transfer, 1982,* **104**, *515–520*

6. **Larson D. W., and Viskanta R.,** Transient combined laminar free convection and radiation in a rectangular enclosure. *J. Fluid Mech., 1976,* **78**, *68–85*

7. **Koutosoheras W. and Charters W. W. S.** Natural convection phenomena in inclined cells with finite side-walls—a numerical solution. *Solar Energy, 1977,* **19**, *433–438*

8. **Meyer B. A., Mitchell J. W., and El-Wakil M. M.** The effect of thermal wall properties on natural convection in inclined rectangular cells. *ASME J. Heat Transfer, 1982,* **104**, *111–117*

9. **Shiralkar G. S. and Tien C. L.** A numerical study of the effect of a vertical temperature difference imposed on a horizontal enclosure. *Numer. Heat Transfer, 1982,* **5**, *185–197*

10. **Kim D. M. and Viskanta R.** Heat transfer by combined wall conduction and natural convection through a rectangular solid with a cavity. *Proceedings of the ASME/JSME Joint Thermal Engineering Conference, (eds Y. Mori and W.-J. Yang), ASME, New York, 1983,* **1**, *313–322*

11. **DeVahl Davis G.** Natural convection of air in a square cavity: A bench mark numerical solution, *University of New South Wales, School of Mechanical and Industrial Engineering Report 1982 (FMT), 1982*

12. **Gartling D. K.** Finite element analysis of several standard flow problems. *Numerical Solutions for a Comparison Problem on Natural Convection in an Enclosed Cavity, (eds. I. P. Jones and C. P. Thompson), AERE-R9955, 1981, 42–53*

13. **Catton I., Ayyaswamy P. S., and Clever R. M.** Natural convection in a finite, rectangular slot arbitrarily oriented with respect to the gravity vector, *Int. J. Heat Mass Transfer, 1974,* **17**, *174–184*

14. **Gilly B., Rox B, and Bontoux P.** Influence of thermal wall conditions on the natural convection in heated cavities. *Numerical Methods in Heat Transfer, (eds. R. W. Lewis, K. Morgan, and B. A. Schrefler), John Wiley & Sons Ltd., London, 1983, Volume II, 205–225*

15. **Wong H. H. and Raithby G. P.** Improved finite difference methods based on a critical evaluation of the approximation errors. *Numer. Heat Transfer, 1979,* **2**, *139–163*

16. **Raithby G. D. and Wong H. H.** Heat transfer by natural convection across vertical air layers. *Numer. Heat Transfer, 1981,* **4**, *447–457*

17. **Roux B., Grodin J. C., Bonrox P. and Gilly B.** On a high-order accurate method for the numerical study of natural convection in a vertical square cavity. *Numer. Heat Transfer, 1978,* **1**, *331–349*

18. **Winters K. H.** Predictions of laminar natural convection in heated cavities. *Numerical Methods in Heat Transfer, (eds. R. W. Lewis, K. Morgan, and B. A. Shrefler), John Wiley & Sons Ltd., London, 1983, Volume II, 179–204*

19. **Davis DeVahl G. and Jones I. P.** Natural convection in a square cavity, a comparison exercise. *Int. J. Numer. Meth. in Fluids, 1983,* **3**, *227–248*

20. **Kuelbeck K., Merker M. P. and Straub J.** Advanced numerical computation of two-dimensional free convection in cavities. *Int. J. Heat Mass Transfer, 1980,* **23**, *203–217*

21. **Eftekhar J., Darkazalli G. and Hai-Sheikh A.** Conduction of heat across rectangular cellular enclosures. *ASME J. Heat Transfer, 1981,* **103**, *591–595*

22, **Naghdi A. K.** Certain heat transfer problems in a rectangular region with multiple cut outs. *Int. J. Heat Mass Transfer, 1983,* **26**, *1143–1149*

23. **Kim D. M.** Heat transfer by combined wall heat conduction convection, and radiation through a solid with a cavity. *Ph.D. Thesis, Purdue University, West Lafayette, Indiana, 1983*

24. **Peaceman D. W. and Rachford H. H., Jr.** The numerical solution of parabolic and elliptic differential equations. *J. Ind. Appl. Math., 1955,* **3**, *28–41*

25. **Roache P. J.** Computational Fluid Dynamics. *Hermosa Publishers, Albuquerque, New Mexico, 1976*

26. **Incropera F. P. and DeWitt D. P.** Fundamentals of heat transfer. *John Wiley and Sons, New York, 1981*

Books received

Physical and Computational Aspects of Convective Heat Transfer, *T. Cebeci and P. Bradshaw*, DM 142 ($55.10 approx.), pp 499, Springer-Verlag

First Parsons International Turbine Conference, £26.00 UK, £32.00 elsewhere, pp 259, Mechanical Engineering Publications

Convection Heat Transfer, *A. Bejan*, £40.85, pp 492, John Wiley & Sons

Particulate Systems: Technology and Fundamentals, *ed J. K. Beddow*, $69.95, pp 373, Hemisphere/McGraw-Hill

Finite Elements in Fluids – Volume 5, *eds R. H. Gallagher, J. T. Oden, O. C. Zienkiewicz, T. Kawai and M. Kawahara*, £37.50, pp 449, John Wiley & Sons

Presents a collection of 19 chapters written by researchers, covering developments and methodologies for applying finite elements to problems of fluid dynamics and heat transfer. Topics include: numerical stability, accuracy, convergence of finite element methods for flow problems, new formulations, and applications to large classes of engineering problems. Theoretical and practical issues are considered.

Measuring Techniques in Gas-Liquid Two-phase Flows, *eds J. M. Delhaye and C. Cognet*, DM 164 ($61.20 approx.), pp 769, Springer-Verlag

Lehrbuch der Reaktortechnik (in German), *A. Ziegler*, DM 48 ($17.90 approx.), pp 307, Springer-Verlag

Advances in Drying (volume 3), *ed A. S. Mujumdar*, DM 164 ($59.70 approx.), pp 372, Hemisphere/Springer-Verlag

The collection of contributed articles presents applied and industrial developments in the art, science and technology of drying. Intended for engineers and scientists involved in drying, the practical relevance of the topic is stressed.

Drying '84, *ed A. S. Mujumdar*, DM 194 ($72.40 approx.), pp 495, Hemisphere/Springer-Verlag

Third compendium volume in this bi-annual series, the book presents recent developments in drying theory and practice. Various topics are covered in 10 sections: international efforts in drying R&D; fundamental studies; freeze drying processes; drying of granular materials; drying of grains; drying of continuous sheets; spray drying; modelling of dryers; novel techniques; and miscellaneous.